Multifrequency, repulsive-mode amplitude-modulated atomic force microscopy

Roger Proksch[a)]
Asylum Research, Santa Barbara, California 93117

(Received 12 May 2006; accepted 13 July 2006; published online 15 September 2006)

An imaging method where a cantilever is driven at or near two of its flexural resonant eigenmodes is described. For most cantilevers, these eigenmodes are nonharmonic. The cantilever and imaging parameters are chosen such that the tip-sample interactions are repulsive. The driven second eigenmode amplitude and phase show strikingly different contrasts from those same fundamental eigenmode signals on graphite samples imaged in air and λ-digest deoxyribonucleic acid samples imaged in water. © *2006 American Institute of Physics*. [DOI: 10.1063/1.2345593]

Since the beginning of atomic force microscopy (AFM), it was recognized that oscillatory techniques were useful.[1,2] Amplitude modulated AFM (AM-AFM)[3] has been applied to a wide variety of materials at high resolution. One active area of research has been in interpreting the phase of the AM-AFM cantilever in terms of the mechanical[4–6] and chemical[7] properties of the surface, with notable progress being made in quantifying energy dissipation.[8,9] However, even with these advances, obtaining quantitative material or chemical properties remains problematic.

During a single AM-AFM vibrational cycle, the tip typically samples a range of forces, from the long range attractive to the short range repulsive. If the tip interacts with the short ranged repulsive forces, information about the mechanical properties of the sample can be obtained. If the periodic repulsive interactions are nonlinear, they will couple energy into higher harmonics,[10–13] which may lead to more information about the mechanical properties of the sample. In addition to the higher harmonics, higher eigenmodes of the cantilever may be excited. The higher modes can also be driven directly. The higher mode amplitude was used as the feedback loop error signal by Stark *et al.*,[14] who also observed enhanced phase contrast on a sample using the third eigenmode of a triangular cantilever.

Sahin *et al.*[15,16] have, through careful cantilever engineering, developed a class of cantilevers whose higher eigenmodes fall on harmonics of the fundamental resonant frequency. They have observed that cantilevers driven at the fundamental exhibit enhanced contrast, based from their simulations on mechanical properties of the sample surface. One challenge of this approach is that it requires cantilevers that are specially manufactured to match an eigenmode with a harmonic.

In some very early work, Martin *et al.*[2] drove the cantilever at two frequencies. The cantilever response at the lower, nonresonant frequency was used as a feedback signal to control the surface tracking and produced a topographic image of the surface. The response at the higher frequency was used to characterize what the authors interpreted as differences in the noncontact forces above the Si and photoresist on a patterned sample.

For single oscillation mode imaging, if the phase shift is positive, it is customary to refer to the imaging mode as "net attractive" or simply "attractive." If the phase shift is negative, the mode is referred to as "repulsive."[17] That convention is adopted here, although any coupling between the eigenmodes may complicate these definitions. Recently, Rodriguez and Garcia[18] published a theoretical simulation of a noncontact, attractive mode technique where the cantilever was driven at its two lowest eigenfrequencies. In their simulations, they observed that the phase of the second mode had a strong dependence on the Hamaker constant of the material being imaged, implying that this technique could be used to extract chemical information about the surfaces being imaged. Crittenden *et al.* have explored using higher harmonics for similar purposes.[19]

This letter presents results of an approach to repulsive mode imaging that keeps some of the benefits of harmonic imaging without requiring the specialized cantilevers of Sahin *et al.* The cantilever is driven at two or more frequencies, chosen to be at or near flexural resonant, generally nonharmonic eigenmodes of the cantilever. In a manner similar to conventional AM-AFM, the amplitude of the cantilever is used as the feedback error signal. Now, however, since there are two or more amplitudes to contend with, there are a number of choices for the feedback loop. The results presented here used the amplitude of the fundamental eigenmode A_1 as the feedback error signal and fundamental phase θ_1, the second eigenmode amplitude A_2, and phase θ_2 as "carry-along" signals. Reversing this and using the higher eigenmode amplitude as a feedback and carrying the fundamental amplitude and phase along also worked well (data not shown). Using the sum of all of the amplitudes as the error signal also allowed stable imaging. An interesting feature of this measurement is that the signal processing can be performed on the same cantilever deflection data stream for each flexural mode. With a digital lock-in implementation, for example, this means that the same position sensitive detector and analog to digital converter (as long as it has sufficient bandwidth for the higher eigenmode) can be used to extract information regarding the distinct eigenmodes.

Figure 1 shows the basic idea of this imaging mode using two typically nonharmonic eigenmodes of a cantilever. The cantilever is driven with a linear combination of sinusoidal voltages, at or near the eigenmodes, f_1 and f_2. This signal is used to drive the base of a cantilever with a "shake" piezo. The experiments reported here were repeated with a magnetically activated cantilever[20] with similar results. It is

[a)]Electronic mail: roger@asylumresearch.com

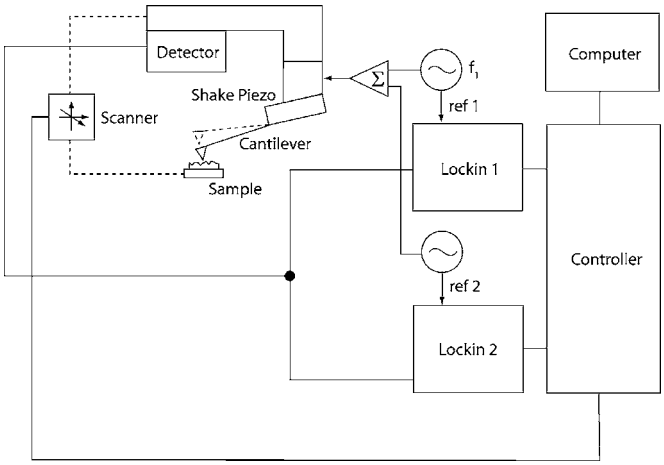

FIG. 1. This shows the experimental apparatus used in this work. The output from two sine wave generators at different frequencies is summed together and then used to drive a "shake piezo" that in turn excites movement in the cantilever. The motion of the cantilever is detected and the signal is fed into two lock-in amplifiers, each referenced to one of the sine waves. The lock-ins outputs are used by the controller to operate feedback loops and are displayed by the computer.

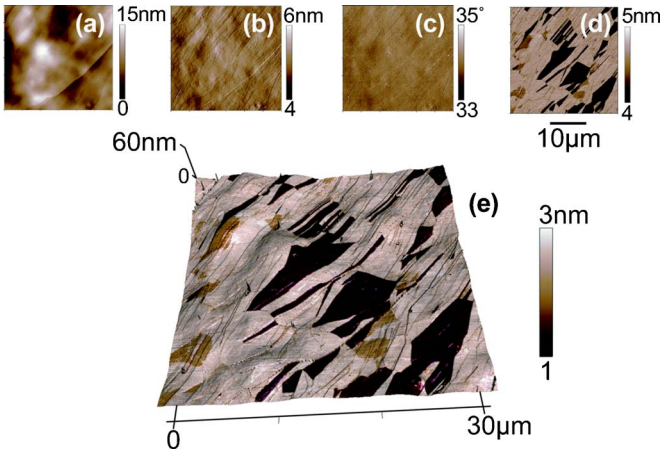

FIG. 2. (Color online) HOPG graphite surface, 30 μm scan. The cantilever was driven at its fundamental (~69.5 kHz) and second eigenfrequency (~405 kHz). (a) shows the topography and (b) is the fundamental amplitude channel, used for the feedback error signal. The fundamental phase image (c) shows an average phase lag of ~34° indicating that the cantilever was in repulsive mode for the entire image. The second mode amplitude is shown in (d). The three dimensional rendered topography colored with the second mode amplitude is shown in (e). This method of display allows easy spatial correlation of the two channels.

expected that other actuation methods where two drive waveforms can be summed will prove as effective. The resulting motion of the cantilever is measured with a position sensor. This signal in turn is used as the input for two separate lock-in amplifiers, where f_1 is used as a reference for one lock-in and f_2 is used as a reference for the other. The output of the lock-in amplifiers, including the Cartesian in-phase and quadrature pairs (x_1, y_1, x_2, y_2) and polar amplitude and phase $(A_1, \theta_1, A_2, \theta_2)$ representations of the cantilever motion at the two or more frequencies can then be passed on to the controller where they can be displayed, saved, combined with other signals, and used in feedback loops. The initial apparatus used a commercially available MFP-3D[21] AFM with an external, home built summing circuit, and an external SR844 lock-in amplifier.[22] Since the initial experiments were performed, a second digital lock-in was implemented on the MFP-3D controller. While the results using this are similar, the signal to noise was improved, probably a result of the simplified signal conditioning on the digital lock-in.

Figure 2 shows a 30 μm image made on a highly oriented pyrolitic graphite (HOPG) surface.[23] The cantilever was a silicon AC-240 cantilever from Olympus. It was driven at the fundamental ($f_1 \sim 69.5$ kHz, $A_1 \sim 8$ nm) and second eigenfrequency ($f_2 \sim 405$ kHz, $A_2 \sim 8$ nm). No significant differences were observed for similar cantilevers imaging the graphite surface. The z-feedback loop was operated using the fundamental amplitude A_1 as the error signal. The topography (a) shows the expected terraces separated by single or multiple atomic steps. The first mode amplitude (b) channel resembles a high-pass filtered image of the topography. The fundamental phase image (c) shows an average phase lag of ~34° and very little variation ($\leqslant 1°$ standard deviation), implying that the cantilever was consistently in repulsive mode. Again, there is very little contrast in this image. The second mode amplitude image (d) however, has significant contrast, with broad patches showing regions where A_2, the second mode amplitude, was reduced by tip-sample interactions. A three dimensional rendering of the surface topography (a) with the second eigenmode amplitude (d) "painted" onto the rendered surface (e) allows the high contrast second mode data to be correlated with the topography. Although (e) makes it clear that there is a high degree of correlation, there are also boundaries in the second mode amplitude that seem to have no connection to topographical features.

A possible explanation of the source of this unusual contrast becomes clear when images were taken different periods of time after initially cleaving the graphite. Initially following cleaving, there were no regions of increased dissipation in the second mode images. After 24 h, however, the high contrast regions apparent in Fig. 2 became visible, consistent with growth of a water layer on different regions of the graphite surface (the relative humidity in the laboratory varied between 40% and 60% during this time). At this point, no systematic study of the growth has been performed. This heterogeneous growth is consistent with some recent electric force microscopy results showing similar variations in the surface potential of freshly cleaved HOPG.[24] It is interesting to note that the high grade HOPG imaged with the technique reported here did not show these regions, only the lower grade with a higher mosaic angle.

Further experimentation with the imaging parameters allowed some similar contrast to be observed in the fundamental eigenmode phase channel (data not shown). The fundamental phase contrast was generally only apparent after first observing the features in second eigenmode image and then fine tuning the fundamental eigenmode imaging parameters. Whereas phase imaging often requires some judicious choice of setpoint and drive amplitude to maximize the phase contrast, this higher modes seem to exhibit high contrast over a much wider range of imaging parameters.

This method of driving the cantilever at two or more resonances works for AM-AFM imaging in fluids as well. A high density λ-digest deoxyribonucleic acid (DNA) sample[25] was prepared in a dense mat on freshly cleaved mica. Figure 3 shows the response of a 60μm long Olympus Bio-Lever in fluid, being driven at its fundamental resonance ($f_1 \sim 8.5$ kHz, $A_1 \sim 8$ nm) and at its second mode (f_2

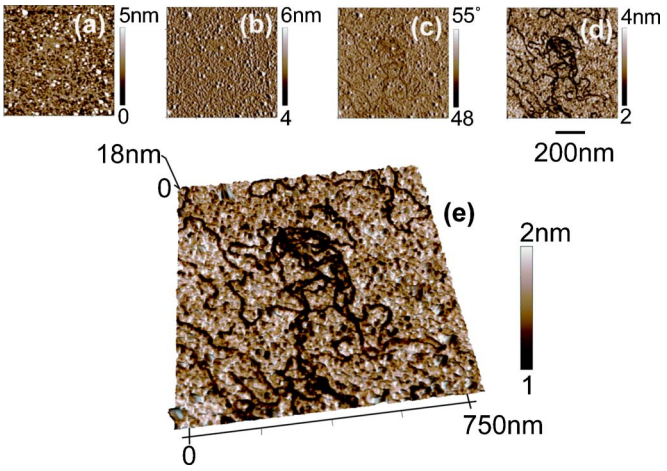

FIG. 3. (Color online) Dense mat of DNA imaged in buffer, 750 nm scan. The 60 μm Bio-Lever was driven at its fundamental resonance (~8.5 kHz) and at its second mode (~55 kHz). The topography (a), fundamental amplitude (b), and fundamental phase (c) all show very little differentiated contrast. The second mode amplitude (d) shows clear, high contrast images of what appear to be strands of DNA molecules. The second mode amplitude was painted onto the three dimensional rendered topography (e) to allow spatial correlation of the two data channels.

~ 55 kHz, $A_2 \sim 5$ nm) in the DNA buffer solution. The topographic image (a) shows a dense mat of material on the surface with no clear strands of DNA visible. Similarly, in the image of the fundamental amplitude (b), the channel used for the feedback error signal shows no particular structure. The fundamental phases channel (c) shows subtle contrast between the background and a structure that shows hints of being strands of DNA molecules. The second mode amplitude (d) shows clear, high contrast images of what appear to be strands of DNA molecules. In this image the strands are dark, corresponding to an increased dissipation at those locations. This is consistent with the DNA strands being slightly less bound to the sample and thus able to absorb some of the second eigenmode energy. Again, rendering the topography in three dimensions and painting the second mode amplitude painted on top (e), allowed these two channels to be spatially correlated.

Despite the promise that phase imaging might prove sensitive to the mechanical and chemical properties of the sample, there are still many problems with the interpretation of these sorts of images. Stark *et al.*[26] specifically showed, for example, that the phase signal can often be linked to simple sample topography or feedback effects rather than to mechanical or chemical sample properties. By measuring the cantilever response at two different frequencies, it is possible to look at the difference in, for example, the phase signals at the fundamental drive frequency and at a higher mode drive frequency. This could help with extracting frequency dependent mechanical properties of the sample.

In closing, significant contrast differences can be observed by operating a repulsive mode AM-AFM cantilever at more than one of its flexural resonances. Driving the cantilever at more than one of its flexural modes allows a rich variety of frequency dependent sample properties to be explored in air or in fluid.

The author thanks Sophia Hohlbach for preparing the DNA sample and Sergei Kalinin for useful discussions and pointing out Ref. 24.

[1] G. Binnig, C. F. Quate, and C. Gerber, Phys. Rev. Lett. **56**, 930 (1986).
[2] Y. Martin, C. C. Williams, and H. K. Wickramasinghe, J. Appl. Phys. **61**, 4723 (1987).
[3] R. Garcia and R. Perez, Surf. Sci. Rep. **47**, 197 (2002).
[4] J. B. Pethica and W. C. Oliver, Phys. Scr., T **T19A** 61 (1987).
[5] R. Garcia, J. Tamayo, and A. San Paulo, Surf. Interface Anal. **27**, 312 (1999).
[6] M. Tello, A. San Paulo, T. R. Rodriguez, M. C. Blanco, and R. Garcia, Ultramicroscopy **97**, 171 (2003).
[7] A. Noy, C. H. Sanders, D. V. Vezenov, S. S. Wong, and C. M. Lieber, Langmuir **14**, 1508 (1998).
[8] J. P. Cleveland, B. Anczykowski, A. E. Schmid, and V. B. Elings, Appl. Phys. Lett. **72**, 2613 (1998).
[9] J. Tamayo and R. Garcia, Appl. Phys. Lett. **73**, 2926 (1998).
[10] M. Stark, R. W. Stark, W. M. Heckl, and R. Guckenberger, Proc. Natl. Acad. Sci. U.S.A. **99**, 8473 (2002).
[11] R. Hillenbrand, M. Stark, and R. Guckenberger, Appl. Phys. Lett. **76**, 3478 (2000).
[12] R. W. Stark and W. M. Heckl, Rev. Sci. Instrum. **74**, 5111 (2003).
[13] R. W. Stark, Nanotechnology **15**, 347 (2004).
[14] R. W. Stark, T. Drobek, and W. M. Heckl, Appl. Phys. Lett. **74**, 3296 (1999).
[15] O. Sahin, G. Yaralioglu, R. Grow, S. F. Zappe, A. Atalar, C. Quate, and O. Solgaard, Sens. Actuators, A **114**, 183 (2004).
[16] O. Sahin, C. F. Quate, O. Solgaard, and A. Atalar, Phys. Rev. B **69**, 165416 (2004).
[17] A. San Paulo and R. Garcia, Phys. Rev. B **66**, 041406 (2002).
[18] T. R. Rodriguez and R. Garcia, Appl. Phys. Lett. **84**, 449 (2004).
[19] S. Crittenden, A. Raman, and R. Reifenberger, Phys. Rev. B **72**, 235422 (2005).
[20] A. Buguin, O. Du Roure, and P. Silberzan, Appl. Phys. Lett. **78**, 2982 (2001).
[21] Asylum Research, Santa Barbara, CA.
[22] Stanford Research Systems, Palo Alto, CA.
[23] HOPG Graphite Grade 1, 2, and 3 SPI Incorporated, West Chester, PA.
[24] Y. Lu, M. Munoz, C. S. Steplecaru, C. Hao, M. Bai, N. Garcia, K. Schindler, and P. Esquinazi, Phys. Rev. Lett. **97**, 076805 (2006).
[25] Sigma 50 ug/ml, imaged in 40 mM HEPES, and 5 mM $NiCl_2$ with a *p*H of 6.6–6.8.
[26] M. Stark, C. Moller, D. J. Muller, and R. Guckenberger, Biophys. J. **80**, 3009 (2001).